

Supplemental Figure Captions

Figure S1. Loss of Bid does not rescue *Atm*^{-/-} spleen size, spermatogenesis defect, splenic T cell defect, or body weight. (A) Number of splenocytes in *Bid*^{+/+}, *Bid*^{-/-}, *Atm*^{-/-}, *BidAtm*^{-/-} mice. (B) Histology of testes in *Bid*^{+/+}, *Bid*^{-/-}, *Atm*^{-/-}, *BidAtm*^{-/-} mice. Both *Atm*^{-/-} and *Bid*^{-/-}*Atm*^{-/-} testes display defective spermatogenesis. (C-E) Immunophenotype analysis of splenocytes in *Bid*^{+/+}, *Bid*^{-/-}, *Atm*^{-/-}, *BidAtm*^{-/-} spleens. Both *Atm*^{-/-} and *Bid*^{-/-}*Atm*^{-/-} spleens display decreased CD4 and CD8 T cells. (D-H). Immunophenotype analysis of splenocytes in *Bid*^{+/+}, *Bid*^{-/-}, *Atm*^{-/-}, *BidAtm*^{-/-} mice. There is no significant difference in the percentage of B220⁺ (pan B cell marker) or CD43⁺ (leukosialin, found on B cells) cells. (I) Weights of *Bid*^{+/+}, *Bid*^{-/-}, *Atm*^{-/-}, *BidAtm*^{-/-} male and female mice. While there is a trend toward smaller body weight for *Bid*^{-/-}, *Atm*^{-/-}, and *Bid*^{-/-}*Atm*^{-/-} mice, most marked in males, these differences do not reach statistical significance.

Figure S2. The lymphoblastic leukemia/lymphoma in *Atm*^{-/-} and *Bid*^{-/-}*Atm*^{-/-} mice displays a similar blast morphology, size of thymic mass, immunophenotype, and organ distribution.

(A) Blast morphology of *Atm*^{-/-} and *Bid*^{-/-}*Atm*^{-/-} lymphoblastic leukemia/lymphoma. Peripheral blood was removed postmortem by cardiac puncture. Blood was smeared onto a microscope slide and stained using the HEMA-3 stat staining kit (Fisher scientific). (B) Weight of thymic masses in leukemic *Atm*^{-/-} and *Bid*^{-/-}*Atm*^{-/-} mice. (C) Immunophenotype of *Atm*^{-/-} and *Bid*^{-/-}

-Atm/- leukemia. The leukemic blasts in both *Atm/-* and *Bid/-Atm/-* mice are CD4⁺CD8⁺ and involve the thymus, spleen, and bone marrow.

Figure S3. Loss of Bid does not rescue T cell differentiation as measured by TCR-β and CD3 expression in *Atm/-* thymocytes. (A) The relative surface expression of TCR-β in both double negative and double positive (DP) populations from *Bid+/+*, *Bid/-*, *Atm/-* and *Bid/-Atm/-* thymi analyzed by flow cytometry. Thymocytes from the indicated genotypes were stained with anti-TCR-β along with anti-CD4, and anti-CD8α. Double positive (CD4⁺CD8⁺, DP) and double negative (CD4⁻CD8⁻, DN) populations were analyzed for TCR-β expression. The TCR-β positive percentages are indicated above (B) Quantitation of the TCR-β positive double positive (DP) cell numbers analyzed from three independent experiments. (C) The surface expression of CD3 in total thymocytes from *Bid+/+*, *Bid/-*, *Atm/-* and *Bid/-Atm/-* mice analyzed by flow cytometry (D) Quantitation of CD3⁺ cell numbers from three independent experiments.

Figure S4. The hematopoietic stem (HSC) and progenitor populations in the bone marrow, their response to IR, and their replating efficiency do not change in *Atm/-* and *Bid/-Atm/-* mice. (A) The frequencies of the HSC-enriched Lineage-negative c-Kit⁺, Sca1⁺ (LSK) and early progenitor (Lineage negative c-Kit⁺ Sca-1⁻) populations from bone marrow of *Bid+/+*, *Bid/-*, *Atm/-* and *Bid/-Atm/-* mice as measured by flow cytometry. (B,C) The cell numbers of progenitor and LSK populations, respectively. (D) *Bid+/+*, *Bid/-*, *Atm/-* and *Bid/-Atm/-* mice were treated with 5Gy ionization radiation for 48 hours and

progenitor and LSK populations were evaluated by flow cytometry (E,F) Cell numbers of progenitor and LSK populations, respectively, 48 hours following 5Gy IR. (G) Serial methylcellulose replating capacity is comparable for *Atm*^{-/-} and *Bid*^{-/-}*Atm*^{-/-} bone marrow. 50,000 cells from whole bone marrow were plated in methylcellulose in the presence of IL3, SCF, IL6, and EPO. Cells were replated every 6 days for a total of 4 platings. The data represents three independent experiments.

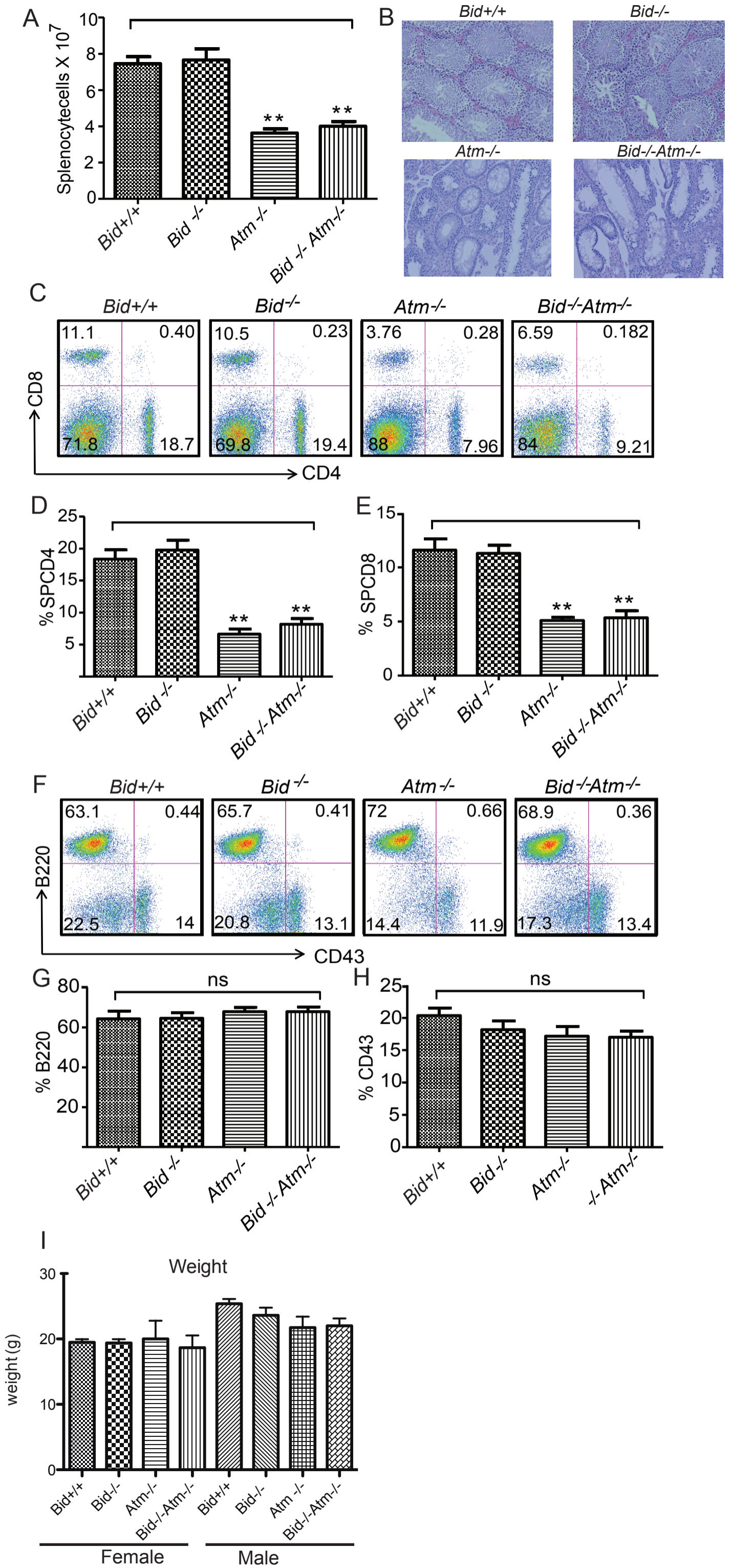
Figure S5. Double Negative 1 (DN1) thymocytes of *Bid*^{+/+}, *Bid*^{-/-}, *Atm*^{-/-} and *Bid*^{-/-}*Atm*^{-/-} mice demonstrate similar proliferation and apoptosis with or without IR treatment (A) BrDU incorporation in DN1 thymocytes of *Bid*^{+/+}, *Bid*^{-/-}, *Atm*^{-/-} and *Bid*^{-/-}*Atm*^{-/-} mice with or without IR treatment. Mice were injected with BrdU three hours prior to sacrifice. BrDU positive (proliferating) cells were detected by intracellular staining with FITC-conjugated anti-BrDU antibody (BD Pharmingen) (B) Quantitation of BrDU positive cells with and without IR. (C) Annexin V positive (apoptotic) DN1 thymocytes of *Bid*^{+/+}, *Bid*^{-/-}, *Atm*^{-/-} and *Bid*^{-/-}*Atm*^{-/-} mice with and without IR. (D) Quantitation of Annexin V staining of DN1 thymocytes with and without IR.

Figure S6. Phosphorylation of the histone γ H2A.X is decreased in *Atm*^{-/-} and *Bid*^{-/-}*Atm*^{-/-} DN3 thymocytes relative to *Bid*^{+/+} and *Bid*^{-/-} DN3 thymocytes following IR. (A) Flow cytometry analysis showing increased phospho-histone γ H2A.X four hours after 5 Gy IR treatment of total *Bid*^{+/+} thymocytes. Thymocytes were stained with surface markers for anti-CD4, anti-

CD8 α , anti-CD44, and anti-Cd25. Then the cells were fixed, permeabilized and incubated with anti-phospho-Histone γ H2A.X (Ser139) (Cell Signaling). Purified IgG1 (EMD Biosciences) was used as an isotype-matched control. (B, C) Relative expression of intracellular γ H2A.X from *Bid*^{+/+}, *Bid*^{-/-}, *Atm*^{-/-} and *Bid*^{-/-} *Atm*^{-/-} DN3 cells without and with IR treatment, respectively.

Figure S7. *Bid*^{+/+}, *Bid*^{-/-}, *Atm*^{-/-} and *Bid*^{-/-} *Atm*^{-/-} DN1 and DN3 thymocytes display similar levels of reactive oxygen species as measured by H₂DCFDA staining. (A-C) H₂DCFDA staining of DN1 and DN3 thymocyte populations from *Bid*^{+/+}, *Bid*^{-/-}, *Atm*^{-/-} and *Bid*^{-/-} *Atm*^{-/-} mice. (D-E) Mean fluorescence (MFI) intensity of H₂DCFDA staining by flow cytometry analysis.

Fig. S1



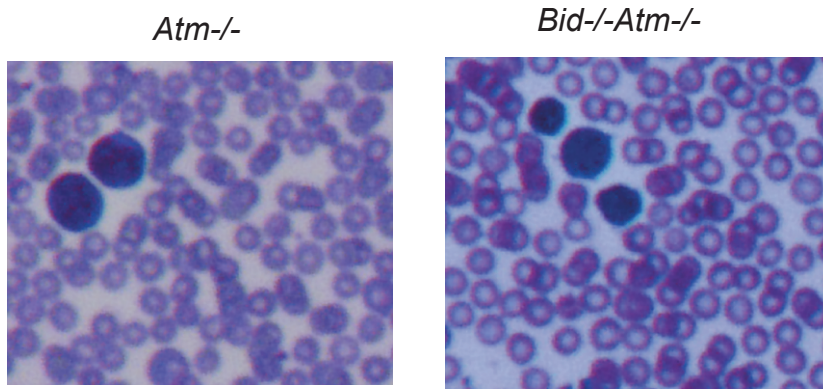
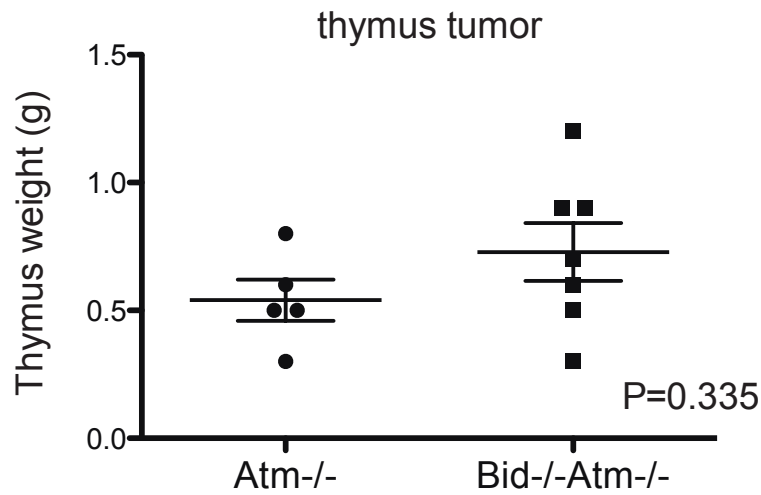
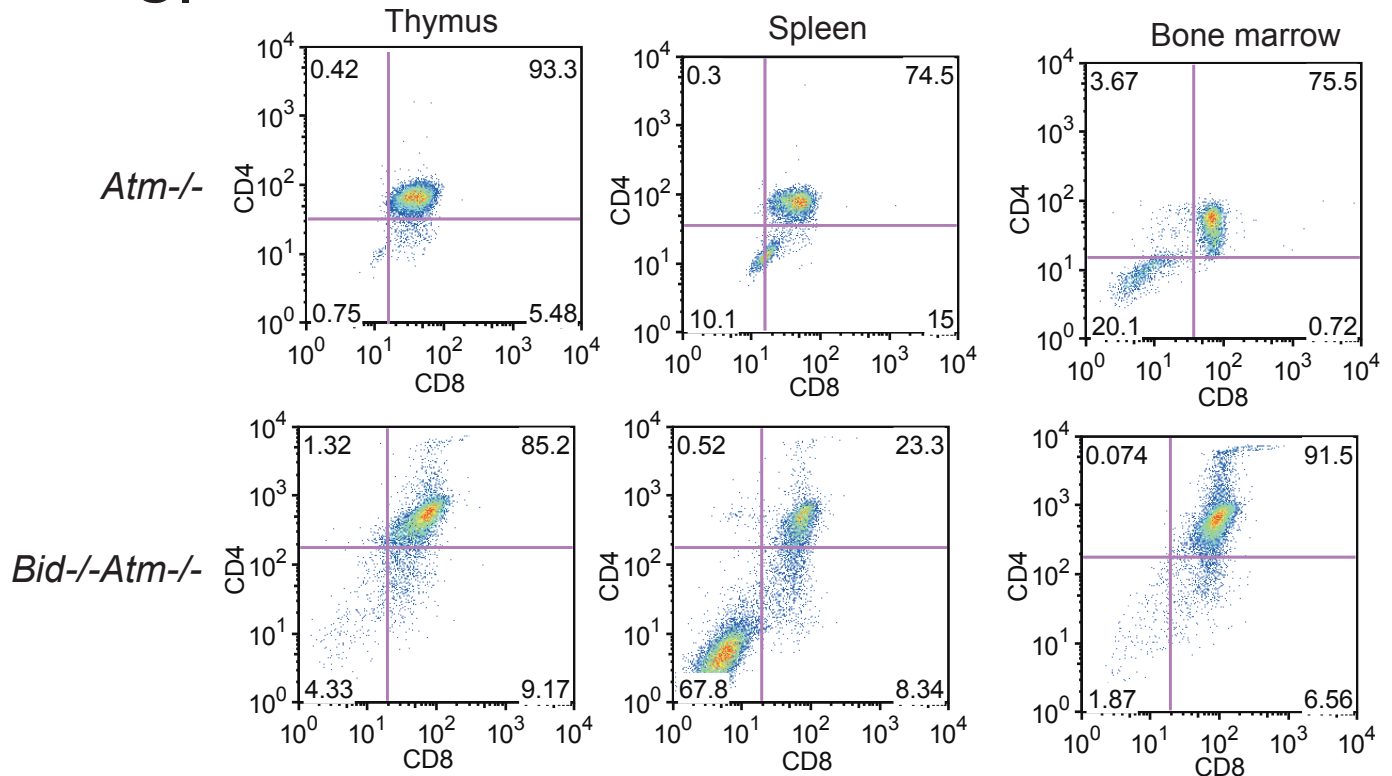
A.**B.****C.**

Fig. S3

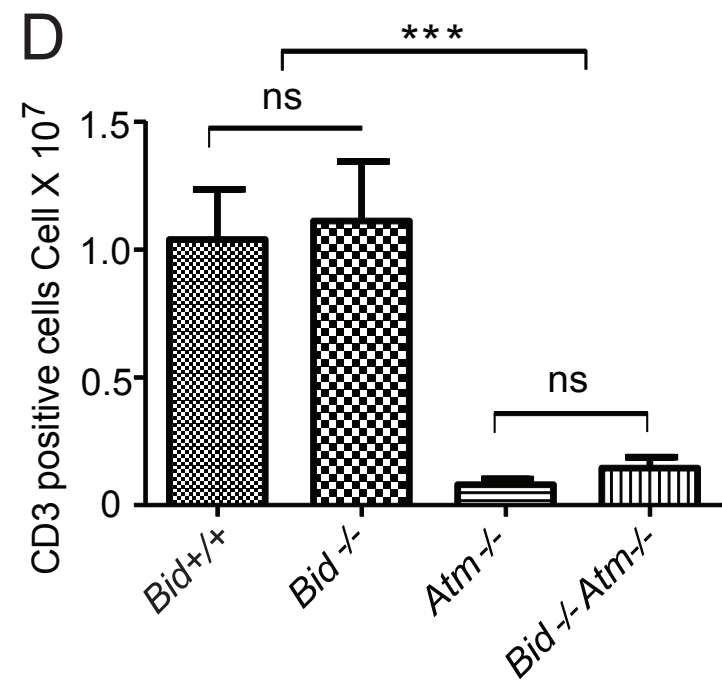
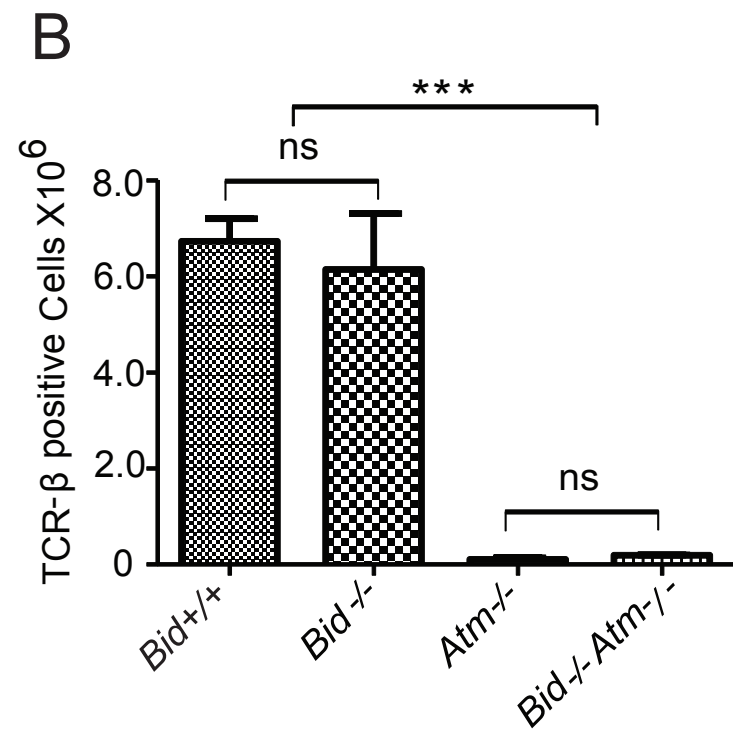
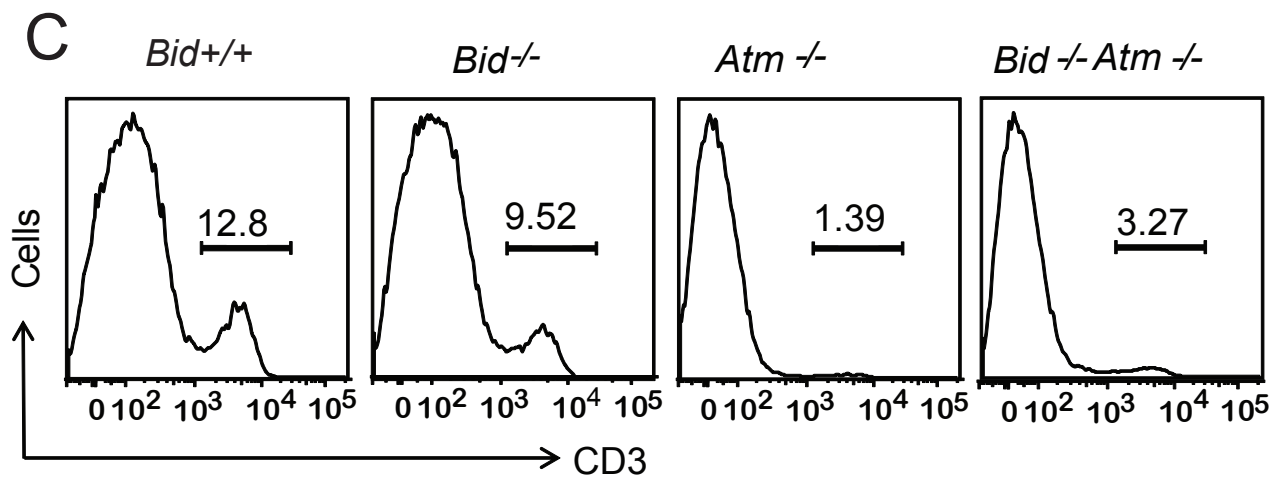
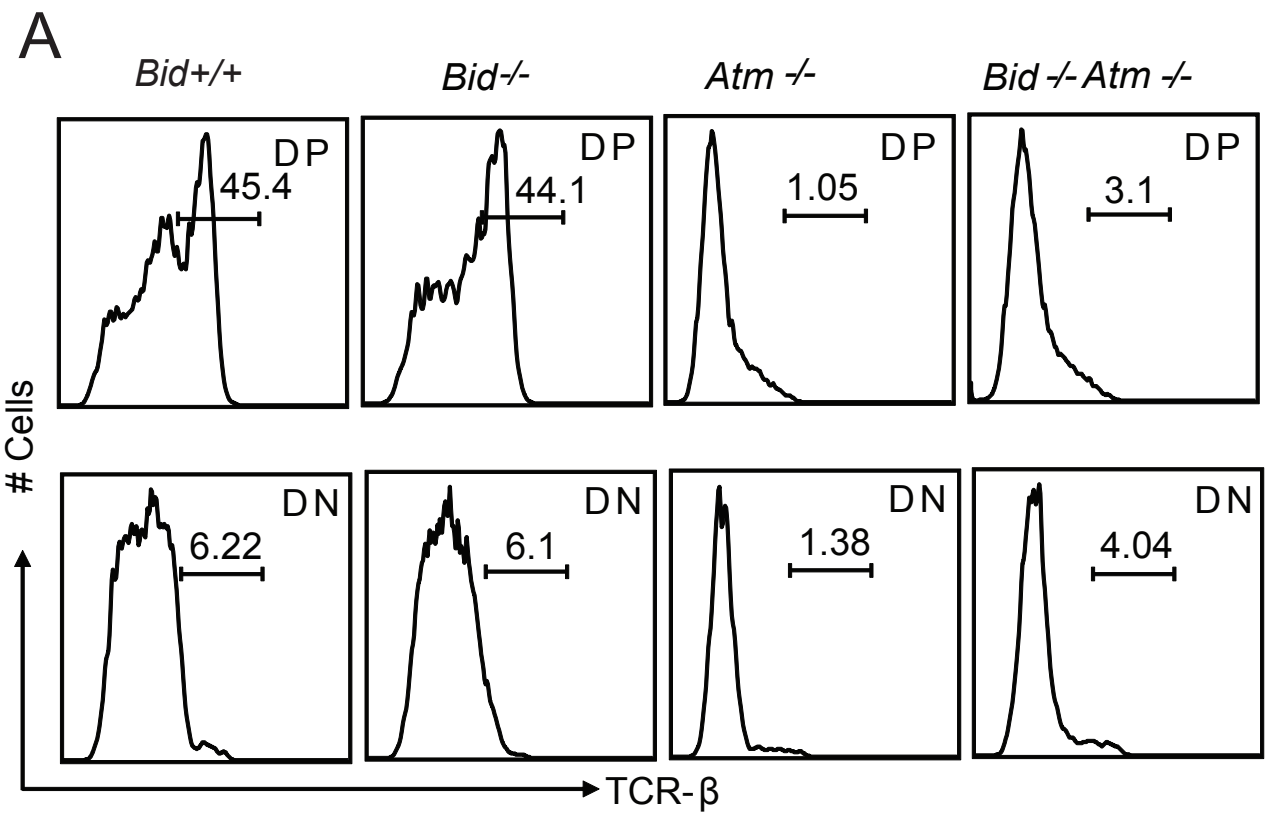


Fig. S4

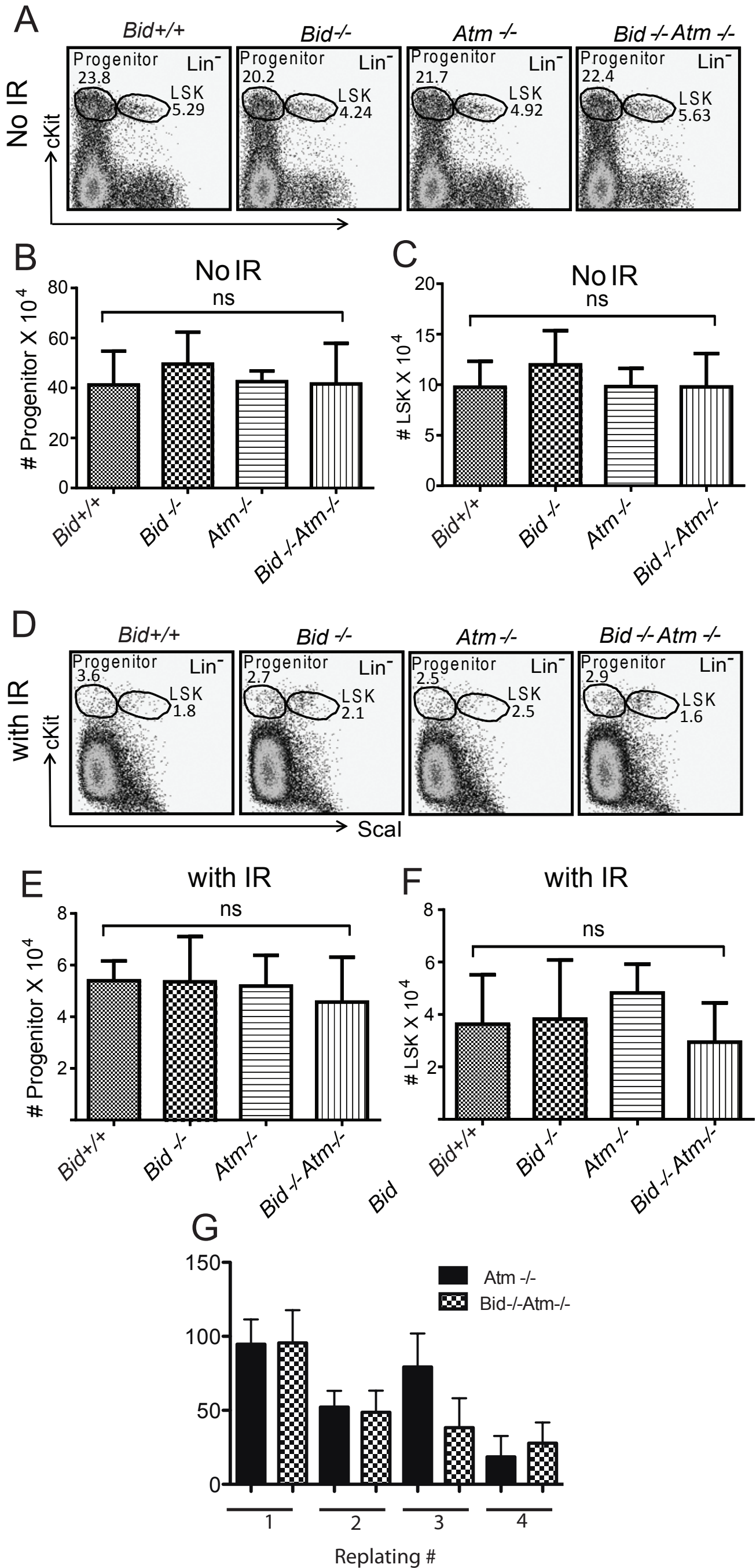


Fig. S5

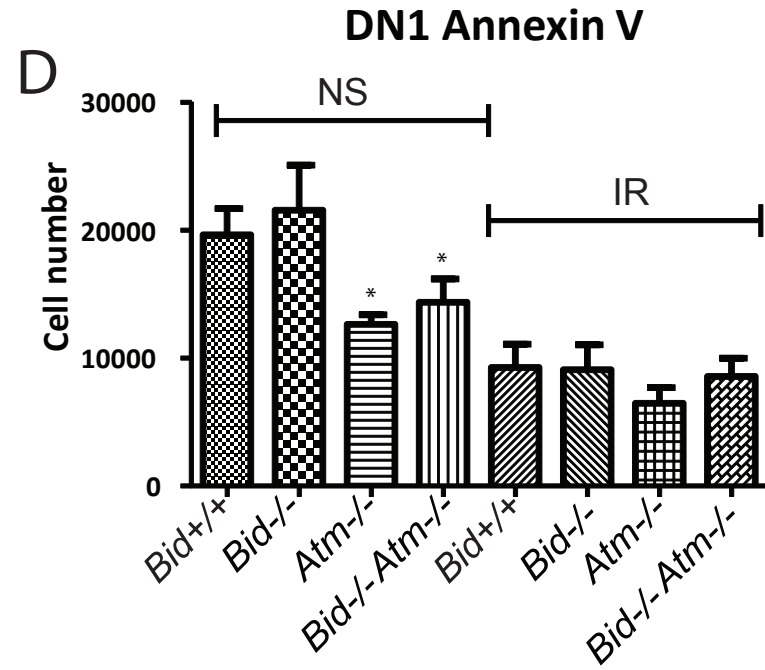
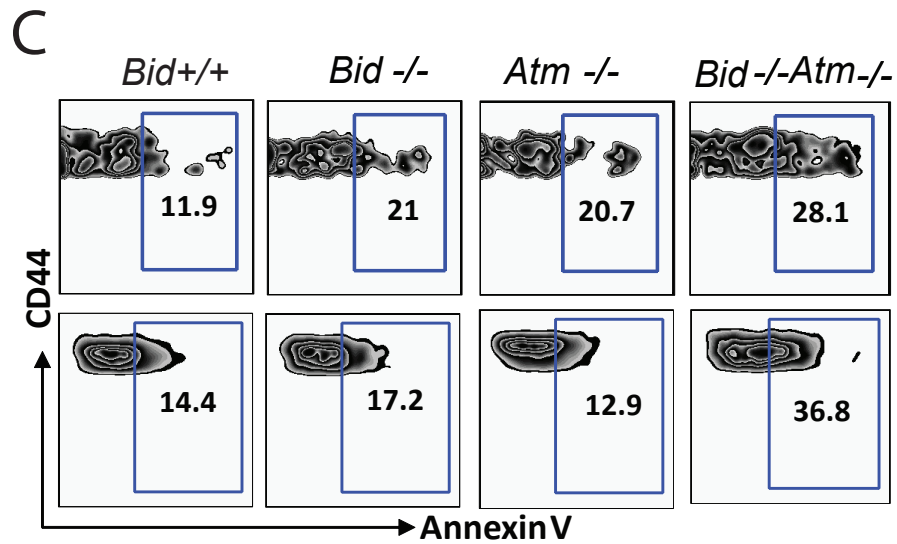
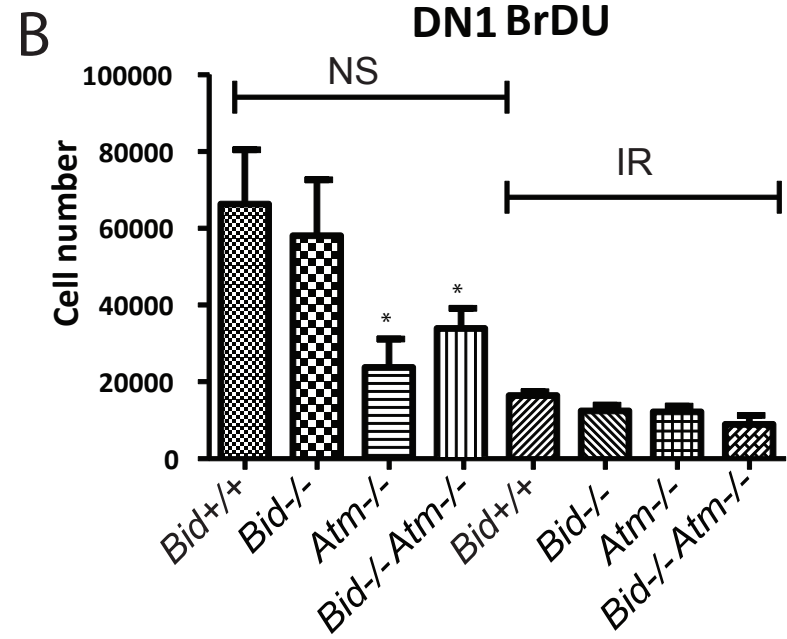
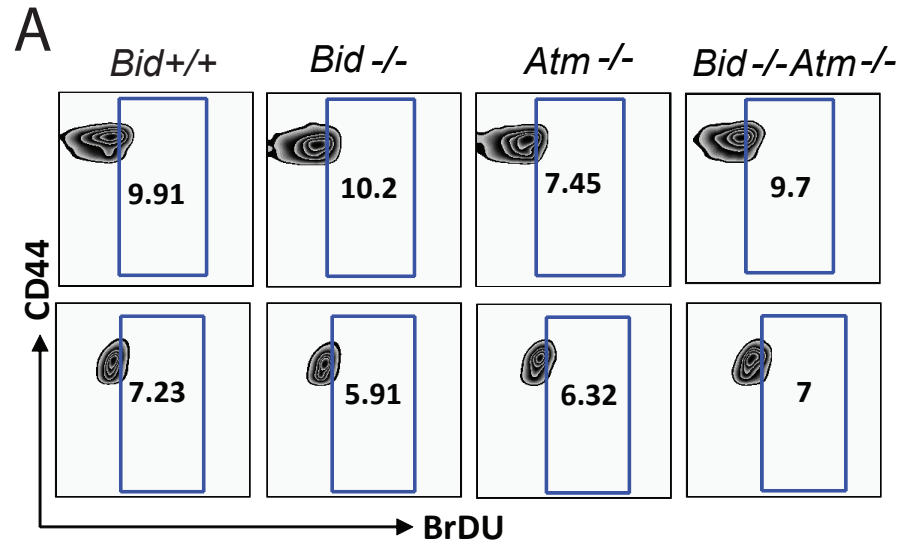
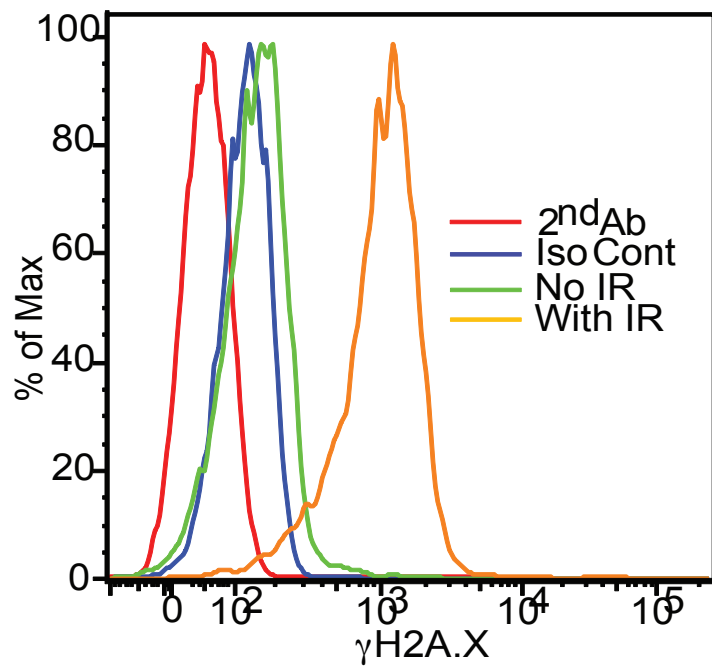
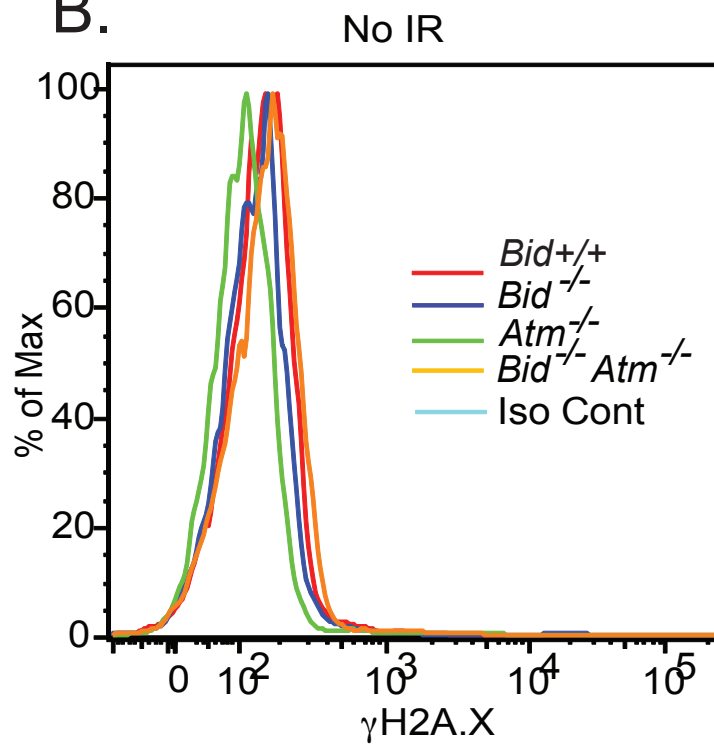


Fig. S6

A.



B.



C.

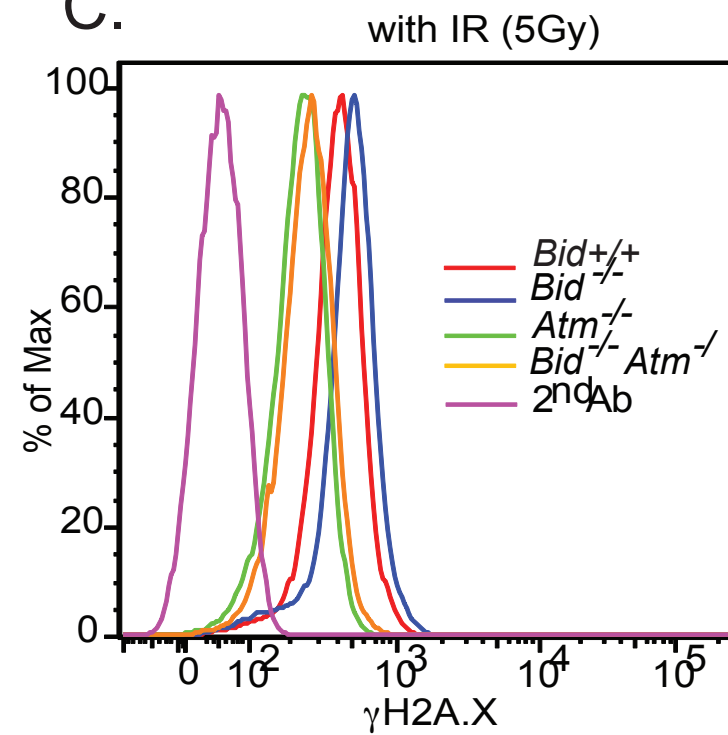


Fig. S7

